

## 5. AMPLITUDE PROBABILITY DISTRIBUTION ANALYSIS

The effect of man-made noise, in the 136 to 138-MHz VHF meteorological satellite band, on radio links can be evaluated through simulation. In this section we describe how we used the noise power measurements to model man-made noise for radio link simulation.

### 5.1 Middleton Noise Model

To simulate man-made noise, it is desirable to first model the noise with analytical representations of the APD using as few statistical parameters as possible (e.g., moments and various measures of “impulsiveness”). To this end, Middleton [15-18] has published a detailed analysis of statistical-physical models of man-made and natural radio noise. This work is lengthy and detailed, consisting of four parts published over a period of more than 4 years.

Middleton’s analysis of non-Gaussian noise is based on the assumption that the noise sources are Poisson distributed in space and time and that “source waveforms” can have random amplitudes, durations, and frequencies. In this work, noise is divided into classes based on the interaction of the time-varying noise voltage and the receiver. Class A noise, composed of Gaussian noise and random pulses, is defined as having a bandwidth that is significantly smaller than the receiver filter of interest (the final IF filter for our purposes). With this assumption, the APD of received instantaneous power  $w$  is:

$$A_1(w) \approx e^{-\gamma T} \sum_{m=0}^{\infty} \frac{(\gamma T)^m}{m!} e^{-w/(2\sigma^2 + m\rho^2)} \quad (5.1)$$

where  $\lambda$  is the mean pulse arrival rate,  $T$  is the mean pulse duration,  $D^2$  is the average pulse power, and  $2F^2$  is the average Gaussian noise power. In this equation the APD depends on the “impulse index”  $\beta$  ( $T$  and not explicitly on  $\lambda$  or  $T$ ). Thus, only three parameters are required to model the ADP of Class A noise. Furthermore, the average received power is roughly proportional to  $\beta T$ ; hence, the IF filter should not affect the shape of the APD as long as its bandwidth is large when compared to the random pulse bandwidth.

Class B noise is defined as having a bandwidth that is larger than the receiver filter of interest. The resultant APD as calculated by Middleton consists of three components: a Gaussian component, a rare event component, and an intermediate event component. The Gaussian and rare event components have the same functional form as Equation (5.1). The intermediate component is much more complicated and includes an infinite series of confluent hypergeometric functions ( $M$ ):

$$A_2(w) = w \sum_{n=0}^{\infty} \frac{(-1)^n A_{\beta}^n}{n!} \Gamma\left(1 + \frac{\beta n}{2}\right) M\left(1 + \frac{\beta n}{2}, 2, -w\right) \quad (5.2)$$

where  $A_{\beta}$  is an “intermediate event impulse index”, and  $\beta$  is known as a “spatial density-propagation parameter” with the restriction  $0 \neq \beta < 2$ . In addition to the three parameters required for  $A_1$  and the

two parameters required for  $A_2$ , another parameter specifying the intersection point for the two functions must be used.

Clearly, the implementation of Equation (5.2) in practical simulations is likely to be onerous. In addition, the determination and implementation of the required six parameters appears to be quite tedious and as noted by Hagn [19], practical parameter estimation techniques deserve considerable additional attention.

Our data represent the noise statistics after the final IF filter in the measurement system. Since the actual receiver bandwidth may differ from the measurement system, it is desirable to simulate the noise process prior to the final IF filter. Determining the parameters that fit Equations (5.1) and (5.2) to our data does not achieve this end. We are able, however, to use these results as a guide in developing noise simulation models from our measurements as described below.

## 5.2 Simplified Noise Model

As indicated above, we were interested in developing a complex baseband, time series representation of the noise process prior to the final IF filter of our measurement system. Following Middleton, we assumed that as observed by the receiver, Class A and Class B noise have a non-Gaussian component with a randomly distributed time of arrival and a Gaussian component that is always present. The Gaussian component is modeled as

$$g_k e^{j\theta_k} \quad (5.3)$$

where  $g_k$  is the Rayleigh-distributed amplitude,  $\theta_k$  is the uniformly distributed phase, and  $k$  is the time index.

The non-Gaussian pulse time of arrival was assumed to be Poisson distributed with pulse arrival rate  $\gamma$ . The probability that one pulse will arrive in  $t$  seconds is  $\gamma t$ , therefore, the presence of a pulse is determined by

$$\chi_k = \begin{cases} 1 & \text{with probability } \gamma \Delta t \\ 0 & \text{with probability } 1 - \gamma \Delta t \end{cases} \quad (5.4)$$

Representations of pulse duration and pulse amplitude differed between Class A and Class B noise. Prior to receiver filtering, the Class A noise was represented by rectangular pulses,  $p_k$ , whose duration corresponded to a bandwidth less than the receiver filter bandwidth. In contrast, prior to receiver filtering, the Class B noise was represented by pulses whose bandwidth exceeded the receiver filter bandwidth.

Class A noise pulse amplitude was characterized by a sudden “step” at low APD exceedence probabilities when plotted on Rayleigh paper. This suggested that a pulse or group of pulses with a constant pulse amplitude was present. Class B noise was characterized by a distribution of amplitudes at low APD exceedence probabilities indicating that a group of pulses with variable pulse

amplitudes was present. When  $w \gg 1$ , the asymptotic expansion of the confluent hypergeometric function in Equation (5.2) yields [20]:

$$A_2(w) \approx \frac{1}{\pi} \sum_{n=0}^{\infty} \frac{(-1)^n}{n!} A_{\beta}^n \Gamma^2(\beta n) \beta n \sin(\pi \beta n) w^{-\beta n} . \quad (5.5)$$

Setting  $\beta \ll 1$  and  $A_{\beta} \ll 1$ , so that only the first few terms of the series are important,  $A_2$  can be approximated using a Weibull APD [21,22]:

$$A_2(w) \approx e^{(-w/w_{ow})^{1/\alpha}} \quad (5.6)$$

where  $w_{ow}$  and  $\alpha$  are the Weibull parameters and

$$\xi \{w\} = w_{ow} \Gamma(\alpha + 1). \quad (5.7)$$

In summary, our complete simplified Class A noise model is

$$\mathbf{v}_k = B e^{j\phi} \sum_{l=1}^{\infty} p_l \chi_{k-l} + \mathbf{g}_k e^{j\theta_k} \quad (5.8)$$

where  $B$  and  $\phi$  are the pulse amplitude and phase. The complete simplified Class B noise model is

$$\mathbf{v}_k = (b_k \chi_k + \mathbf{g}_k) e^{j\theta_k} , \quad (5.9)$$

where  $b_k$  is the Weibull distributed amplitude of the non-Gaussian noise component.

The Weibull distributed amplitude is generated by

$$b_k = \sqrt{w_{ow}} (-\log_e u_k)^{\alpha/2} , \quad (5.10)$$

where  $u_k$  is a uniformly distributed random variable with a range from 0 to 1. In a similar way the Rayleigh distributed amplitude was generated by

$$b_k = \sqrt{w_{og}} (-\log_e u_k)^{1/2} , \quad (5.11)$$

where  $w_{og}$  is the mean Gaussian power.

A number of our measurements show that in addition to impulsive noise, there were “constant” noise sources with bandwidths narrower than our IF filter. The constant noise may originate from periodic, pulsed emissions from nearby electrical and electronic equipment. The constant noise component was characterized by a decrease in the slope of the straight line at high APD exceedence probabilities. These noise sources were modeled by adding a constant to the Gaussian noise component

$$z_k = g_k e^{j\theta_k} + c \quad (5.12)$$

where  $c$  is a constant. The amplitude of the resulting variate is Nakagami-Rice distributed

$$p(|z|) = 2|z|(1 + K)\exp(-|z|^2[1 + K] - K) I_0(2|z|\sqrt{K[1 + K]}) \quad (5.13)$$

where

$$K = \frac{|E\{z\}|^2}{E\{|z - E\{z\}|^2\}} = \frac{|c|^2}{w_{og}} \quad (5.14)$$

is the ratio of constant noise-power to Gaussian noise-power. When plotted on Rayleigh paper, the Nakagami-Rice cumulative distribution function is approximately a straight line with a slope that depends on the  $K$  (see e.g., Figure 2.6).

### 5.3 Extraction of Noise Model Parameters from Measurements

The APD's used for simulation were composed of several measured histograms from each environment. Combining histograms was necessary to increase the accuracy of the low exceedence probability estimates. For most of our measurements  $w_{og}$  was estimated readily from the APD's 37th percentile amplitude. For Class A noise two additional parameters were extracted from the APD:  $T$  and  $B$ . For Class B noise, three additional parameters were required for each Poisson/Weibull process:  $T$ ,  $\mu$ , and  $w_{ow}$ .

The product  $\mu T$  is estimated from the APD exceedence probability associated with a departure from a Rayleigh distribution. The parameter  $\mu$  was calculated from the product  $\mu T$  after  $T$  was measured or estimated. For Class A noise we assumed  $T$  was much greater than the receiver filter time constant, therefore, the  $T$  before and after the receiver filter was the same. For Class B noise, prior to filtering, the pulse was assumed to be an impulse. After filtering, the pulse duration was estimated to be the duration of a unit amplitude, rectangular pulse with approximately the same area as the filter impulse response.

The constant amplitude of Class A noise was read directly from the amplitude of the low exceedence probabilities of the APD. The Weibull distribution parameters  $\mu$  and  $w_{ow}$  of Class B noise are ideally estimated from the slope and amplitude of the lower exceedence probability events whose event spacing is much greater than the filter time constant. In practice, for many of the Class B

APD's, there was not sufficient data to measure  $\mu$ . In these cases,  $\mu$  was adjusted empirically to provide the best fit.

Using the estimated parameters, the simulated time series was passed through a digital implementation of our noise measurement receiver final IF filter, and the resultant APD was compared with the measured APD. It was found that, except for  $w_{og}$ , several iterations were required to determine the optimum parameter values.

## 5.4 Simulation Results

For our analysis, we selected measurements that covered a variety of man-made noise environments. These APD's represent typical examples of first-order statistics for a particular measurement location or environment. From the representative noise measurements in Section 3 only the rural environment and computer APD's have been excluded. The rural environment was excluded because it was the quietest environment. The computer APD was excluded because it was similar to the Nakagami-Rice APD found in the office park. As indicated above, these Class A and Class B noise parameters characterize noise before the final IF filter of the measurement system. The simulated APD's shown in Figures 5.1 through 5.18 were filtered by a six-pole Chebychev filter with a 34-kHz noise equivalent bandwidth which approximated our noise measurement receiver filter. A 10- $\mu$ s time increment was used. In the following discussion  $w_o = E\{w\}$ ,  $W_o = 10\log_{10}(w_o)$ ,  $W_{og} = 10\log_{10}(w_{og})$  and  $W_{ow} = 10\log_{10}(w_{ow})$ .

Figure 5.1 shows an example of a Class A noise APD. For this simulation, the Class A noise pulse duration is 1.0 ms, pulse arrival rate is 0.3 pulses/second, and the pulse amplitude is 67.0 dB above  $kT_o b$ . Class B noise also is included in this simulation. The Class B noise parameters are  $\mu = 1.0$ ,  $\bar{c} = 30.0$  pulses/second, and  $W_{og} = 7.3$  dB,  $W_{ow} = 27.0$  dB,  $W_o = 33.4$  dB above  $kT_o b$ . Class A noise with large amplitudes was observed at many of our measurement sites. The time between Class A noise events, however, was on the order of hours, and the duration of the events was less than 100 ms. Since our measurements indicated that Class A events are rare and of short duration, the remainder of our analysis focused on the simulation of the more common Class B noise.

In Table 2 we have tabulated the simulation parameters for Class B noise corresponding to several man-made noise locations and sources. Figures 5.2 through 5.16 show the comparison between the measured and simulated APDs for each entry in Table 2. Note that in some cases, two non-Gaussian noise components are required to obtain a suitable APD. This may be the case, for example, when both strong power line and automotive noise sources are present.

Figures 5.17 and 5.18 show Nakagami-Rice distributed APD's from the office park measurements. Electrical or electronics equipment with periodic, pulsed emissions may be a source of constant narrowband noise. The Class B and Nakagami-Rice parameters for Figure 5.17 are  $K = 3.0$  dB,  $\mu = 2.0$ ,  $\bar{c} = 0.8$  pulses/second, and  $W_{og} = 11.0$  dB,  $W_{ow} = 32.0$  dB,  $W_o = 14.5$  dB above  $kT_o b$ . The Class B and Nakagami-Rice parameters for Figure 5.18 are  $K = 3.0$  dB,  $\mu = 2.0$ ,  $\bar{c} = 10.0$  pulses/second,

and  $W_{og} = 11.0$  dB,  $W_{ow} = 32.5$  dB,  $W_o = 14.7$  dB above  $kT_o b$ . Figure 3.3b shows the median, mean, and peak power for this time and location.

### 5.5 Change of Simulation Time Increment

When performing Class B noise simulations, the average power of the non-Gaussian component depends on the time increment as follows:

$$\langle W_{ow}(dB/kT_o) \rangle = W_{ow}(dB/kT_o) + 10 \log_{10}(\gamma \Delta t) . \quad (5.15)$$

where  $\Delta t$  is the simulation time increment. The tacit assumption in our model is that prior to the final IF filter, Class B noise can be treated as a series of pulses having a duration less than  $\Delta t$ . The  $\Delta t$  for a particular receiver analysis would, of course, be based on the bandwidth of the receiver IF filter.

To determine  $W_{ow}$  for a different time increment the average powers of the non-Gaussian processes are equated at the two time increments, and therefore

$$W'_{ow}(dB/kT_o) = W_{ow}(dB/kT_o) + 10 \log_{10}(\Delta t / \Delta t') \quad (5.16)$$

where the prime denotes  $\Delta t$  and  $W_{ow}$  values at the new time increment.

Table 2 Simulation Parameters for Various Noise Environments

Related Figures	Location	Environment or Source	Date mm/dd/yy	Time hh:mm	C pulses/s	"	$W_{ow}$ dB relative to $kT_0^*$	$W_{og}$ dB relative to $kT_0$	$W_o$ dB relative to $kT_0$
5.2 3.1a	Lakewood, Colorado	Residential	11/10/96	12:00 a.m. 12:40 a.m.	220.0	0.5	31.0	4.6	6.9
5.3 3.1a	Lakewood, Colorado	Residential	11/10/96	3:30 p.m. 4:00 p.m.	220.0 2.0	0.5 0.5	23.0 62.0	5.1	15.0
5.4 3.1b	Lakewood, Colorado	Residential	11/11/96	12:16 p.m. 12:46 p.m.	1.5	3.0	43.0	4.6	5.6
5.5 3.2a	Boulder, Colorado	Residential	11/16/96	12:00 a.m. 12:30 a.m.	30.0	3.0	18.0	3.2	3.4
5.6 3.2b	Boulder, Colorado	Residential	11/17/96	9:00 a.m. 9:30 a.m.	1500.0 3.0	0.75 1.0	32.0 43.0	5.0	13.5
5.7 3.3a	Office park near highway	Light Urban	11/25/96	12:00 a.m. 1:00 a.m.	220.0 4.5	0.5 3.5	19.0 20.0	6.2	6.4
5.8 3.3a	Office Park near highway	Light Urban	11/25/96	12:00 p.m. 12:30 p.m.	30.0	3.5	19.0	8.3	8.6
5.9 3.3c	Office park near residential	Light Urban	11/30/96	12:00 a.m. 1:00 a.m.	2.0	5.0	25.0	5.7	5.8

Table 2, cont., Simulation Parameters for Various Noise Environments

Related Figures	Location	Environment or Source	Date mm/dd/yy	Time hh:mm	$\zeta$ pulses/s	"	$W_{ow}$ dB relative to $kT_0$ *	$W_{og}$ dB relative to $kT_0$	$W_o$ dB relative to $kT_0$
5.10 3.3c	Office park near residential	Business	11/30/96	1:00 p.m. 1:30 p.m.	25.0	4.0	22.0	6.6	7.2
5.11 3.4a	Downtown Boulder, Colorado	Business	11/20/96	1:00 p.m. 1:30 p.m.	150.0	2.5	30.0	18.0	18.5
5.12 3.4b	Downtown Denver, Colorado	Business	12/03/96	11:00 a.m. 11:30 a.m.	25.0	3.0	34.0	19.0	19.1
5.13 3.4b	Downtown Denver, Colorado	Business	12/03/96	11:20 a.m. 11:50 a.m.	60.0	2.5	35.0	19.0	19.4
5.14 3.6	Clear Creek Canyon, Colorado	Automotive	12/21/96	1:00 p.m. 1:30 p.m.	25.0	3.0	15.0	5.5	5.5
5.15 3.6	Clear Creek Canyon, Colorado	Automotive	12/21/96	2:00 p.m. 2:30 p.m.	15.0	6.0	16.0	5.3	6.3
5.16 3.7	Leyden, Colorado	Electrical Network	11/12/96	2:02 p.m.	495.0	0.5	46.0	5.0	22.6

\* depends on the time increment of the simulation (see equation 5.15).

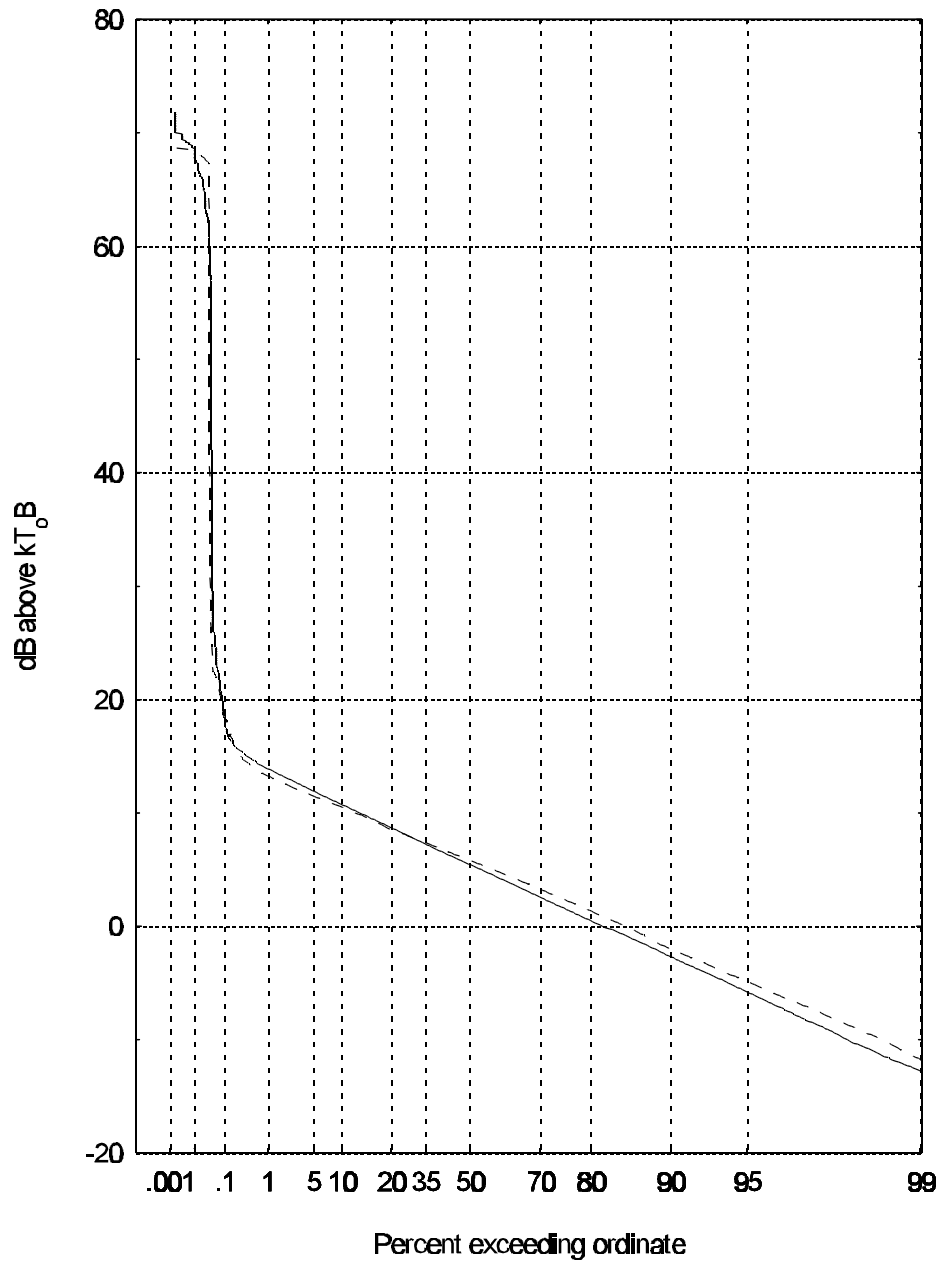


Figure 5.1 Class A noise from measurements at Plainview Open Space site near Boulder, Colorado, on November 7, 1996, at 3:11 p.m.

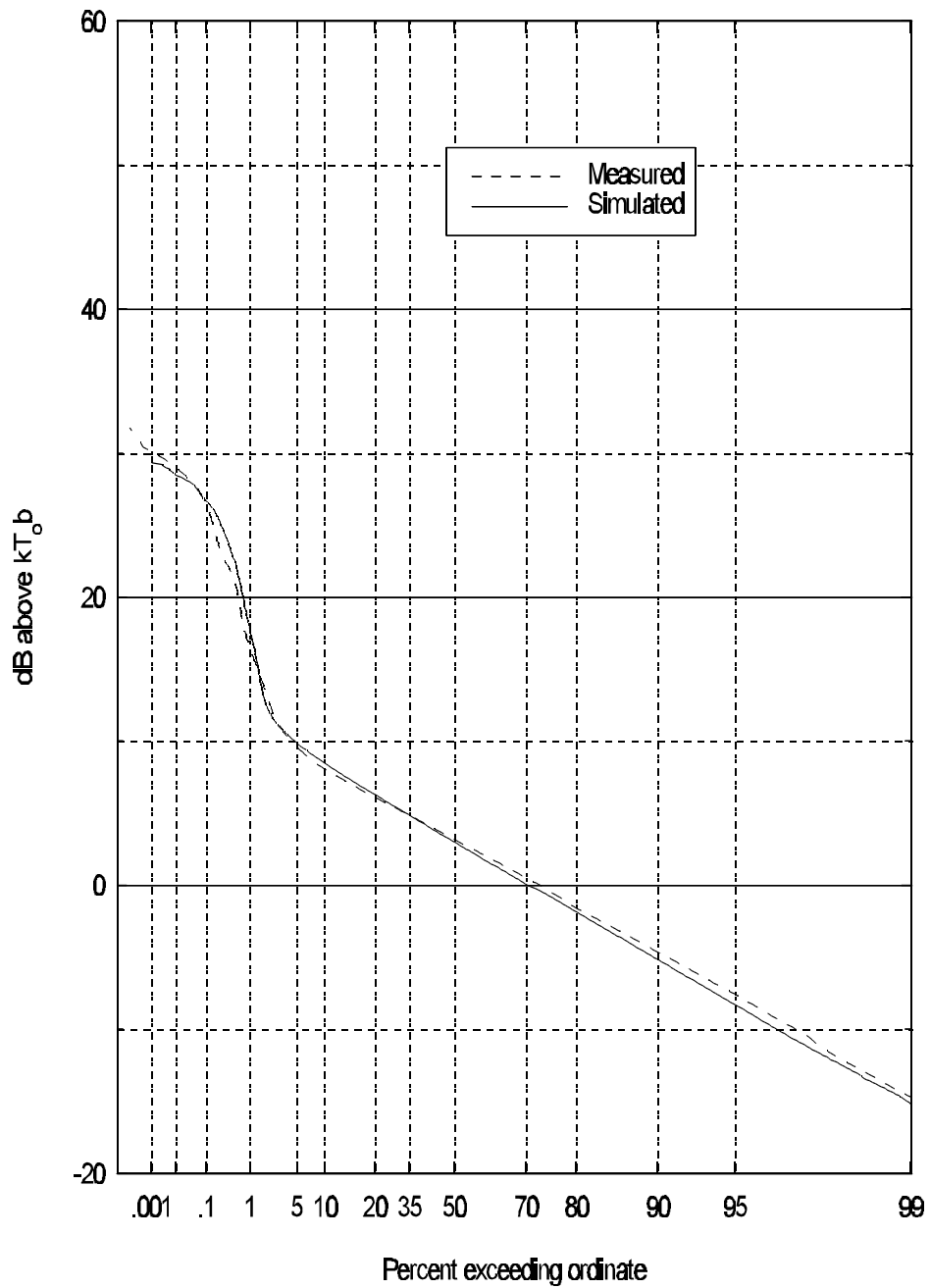


Figure 5.2 Class B noise from measurements at Lakewood, Colorado, residence on November 10, 1996, from 12:00 to 12:40 a.m.

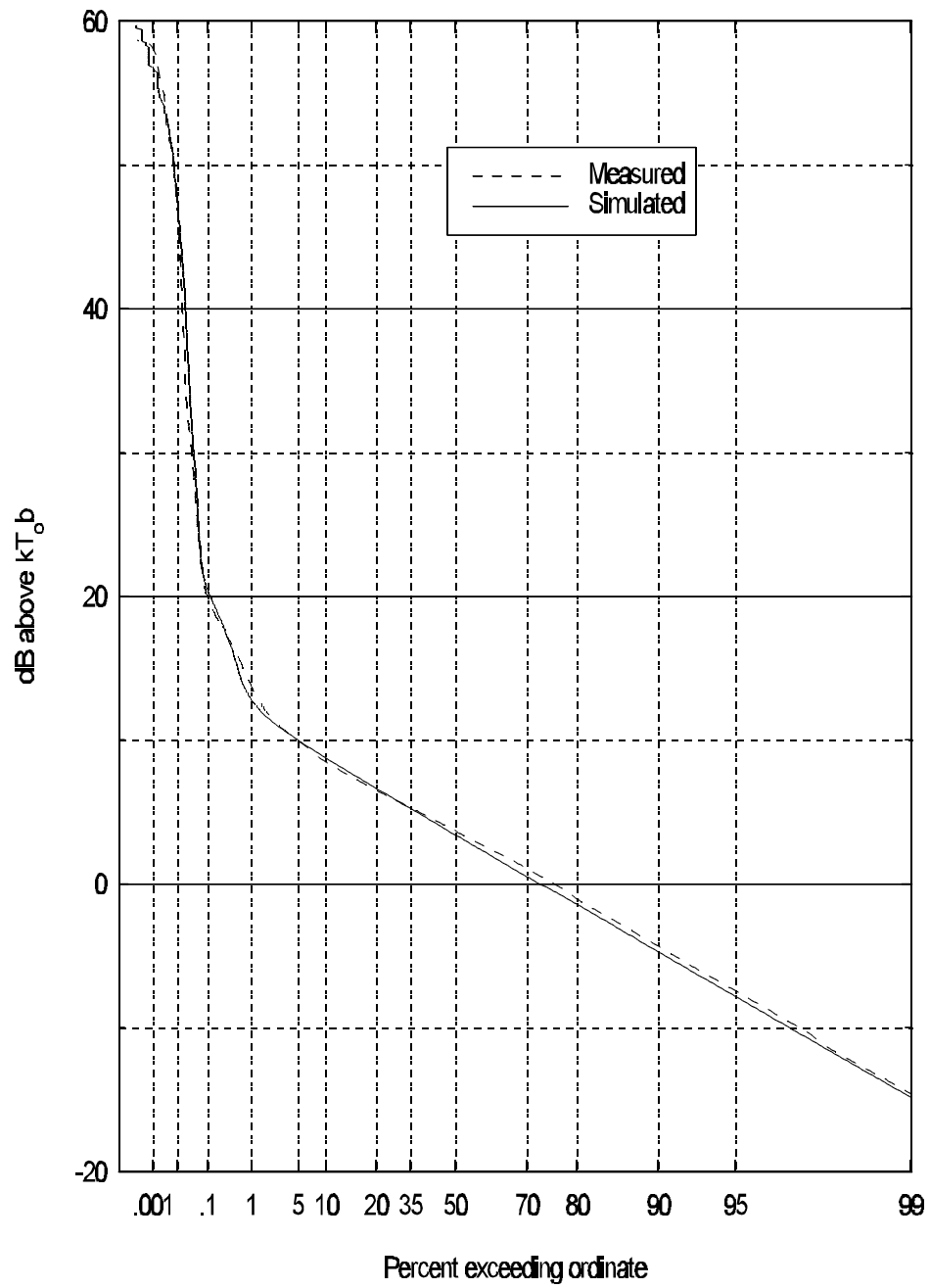


Figure 5.3 Class B noise from measurements at Lakewood, Colorado, residence on November 10, 1996, from 3:30 to 4:00 p.m.

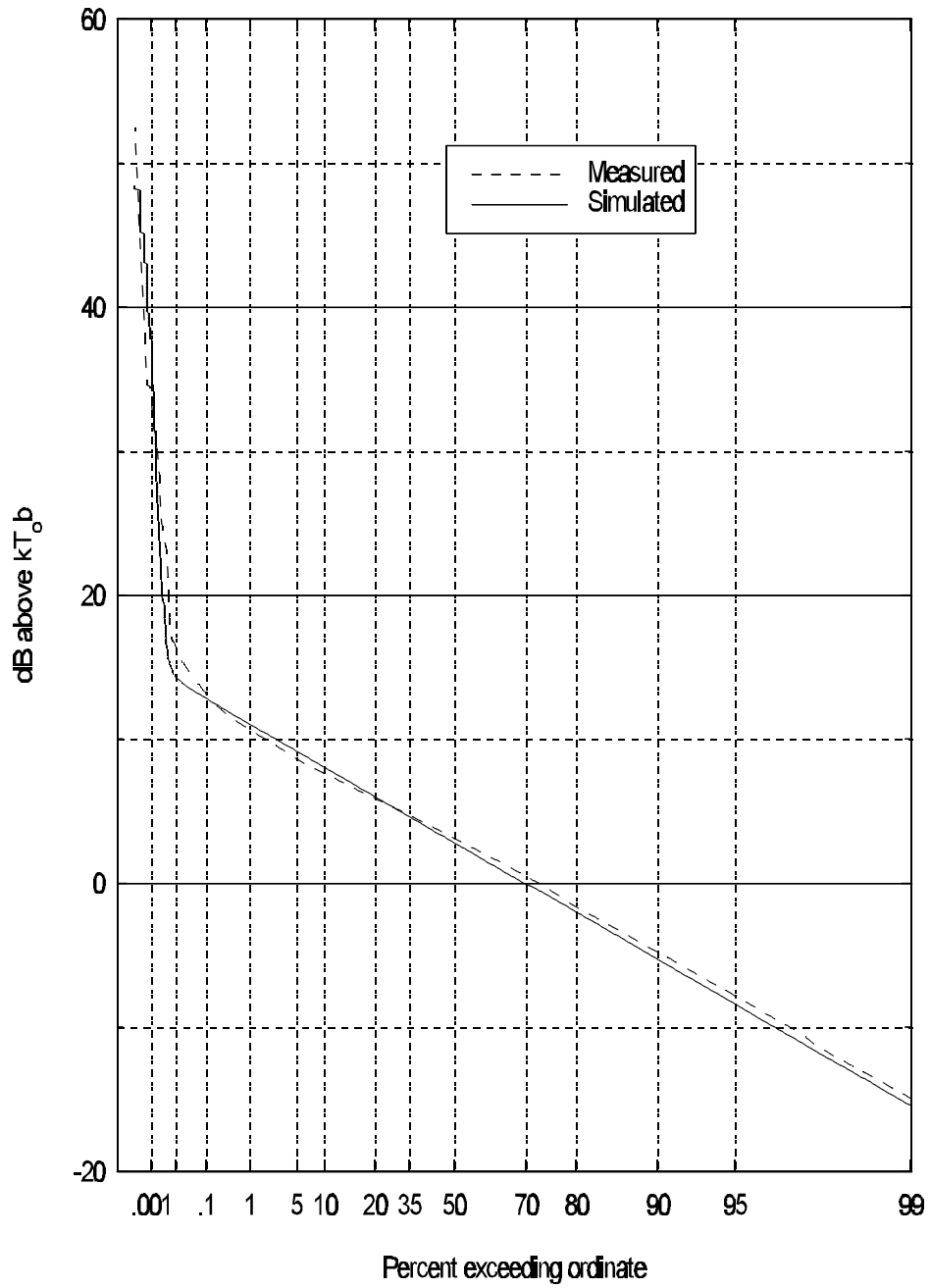


Figure 5.4 Class B noise from measurements at Lakewood, Colorado, residence on November 11, 1996, from 12:16 to 12:46 p.m.

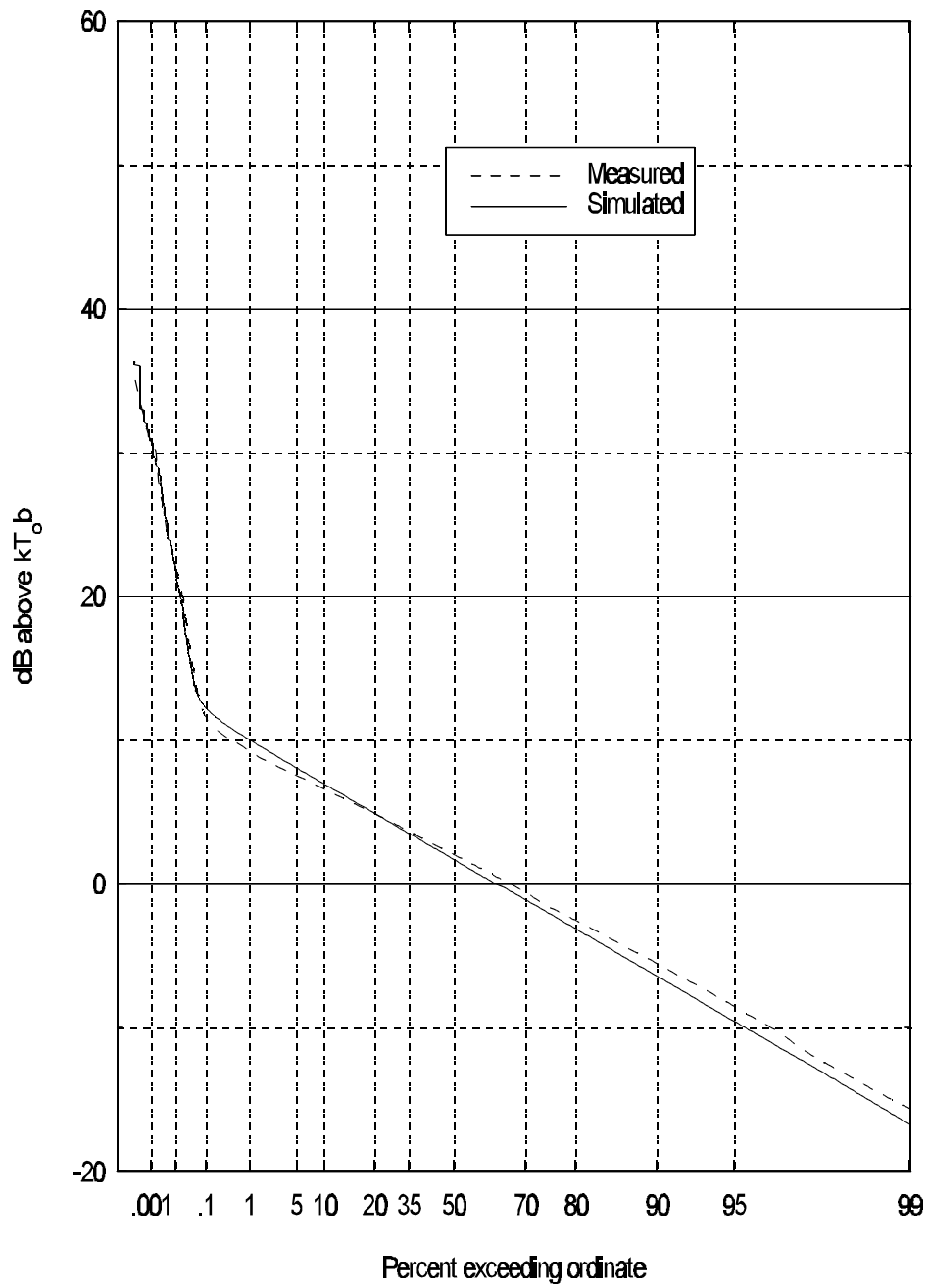


Figure 5.5 Class B noise from measurements at Boulder, Colorado, residence on November 16, 1996, from 12:00 to 12:30 a.m.

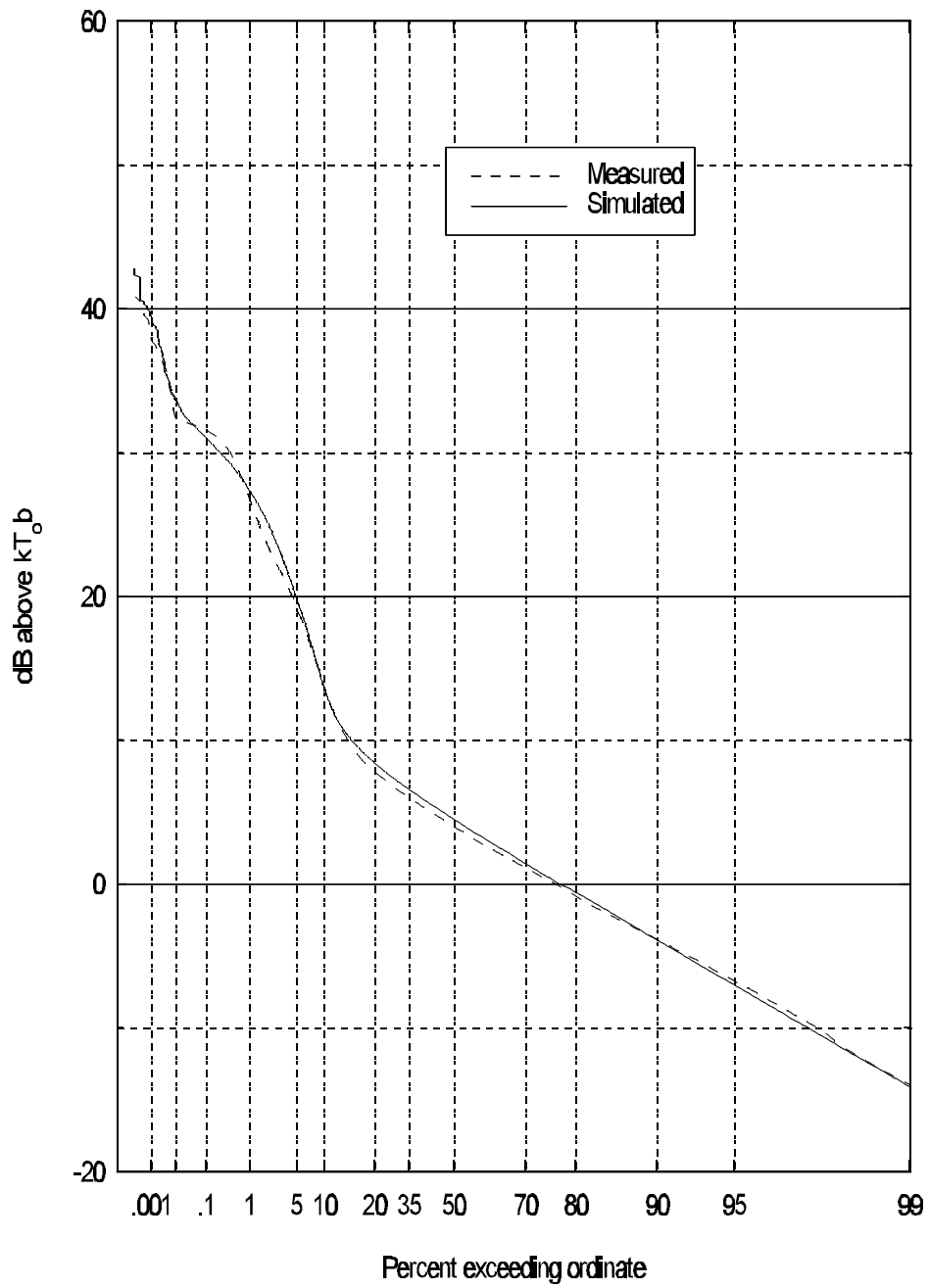


Figure 5.6 Class B noise from measurements at Boulder, Colorado, residence on November 17, 1996, from 9:00 to 9:30 a.m.

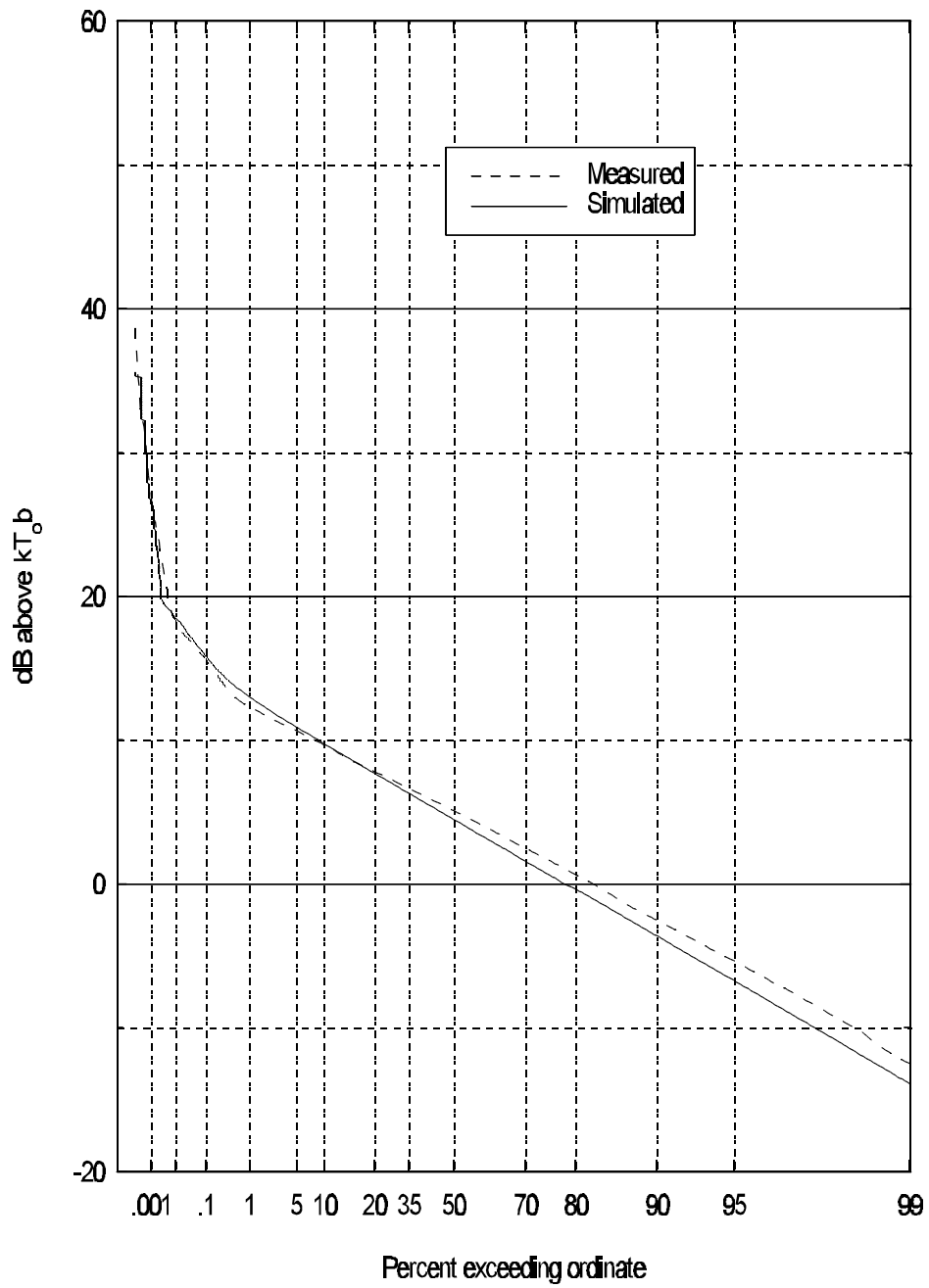


Figure 5.7 Class B noise from measurements in office park on November 25, 1996, from 12:00 to 1:00 a.m.

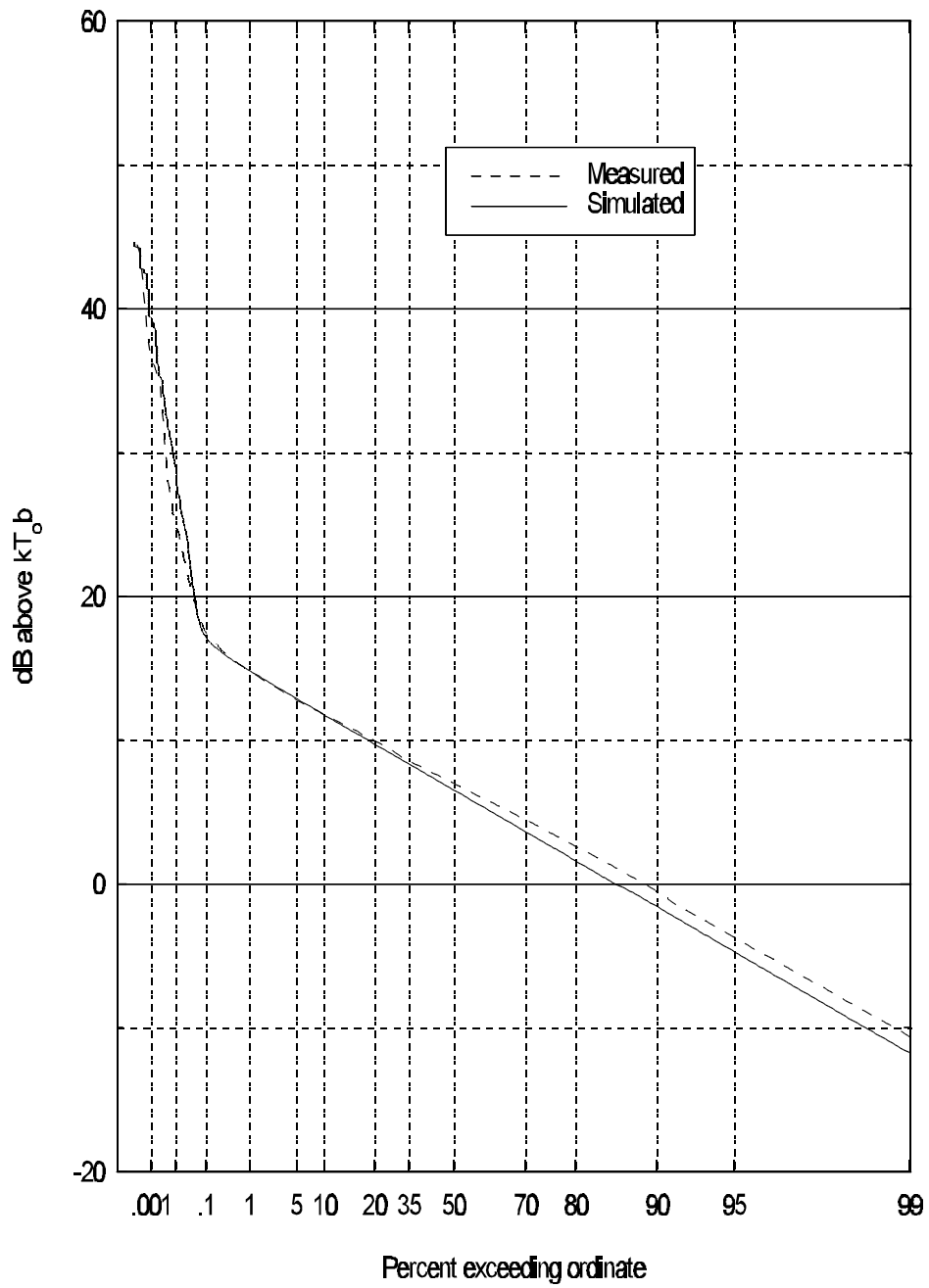


Figure 5.8 Class B noise from measurements in office park on November 25, 1996, from 12:00 to 12:30 p.m.

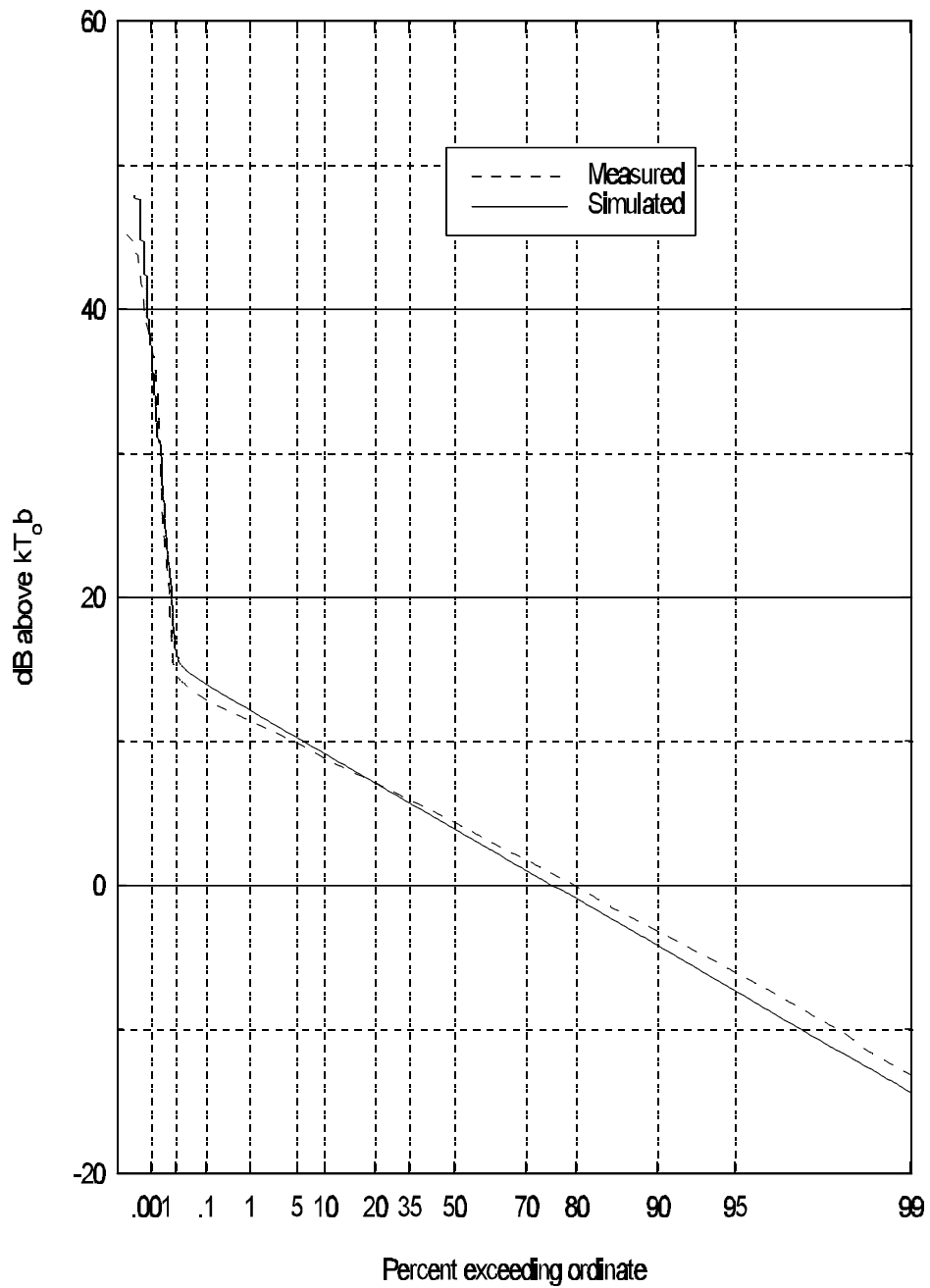


Figure 5.9 Class B noise from measurements in office park on November 30, 1996, from 12:00 to 1:00 a.m.

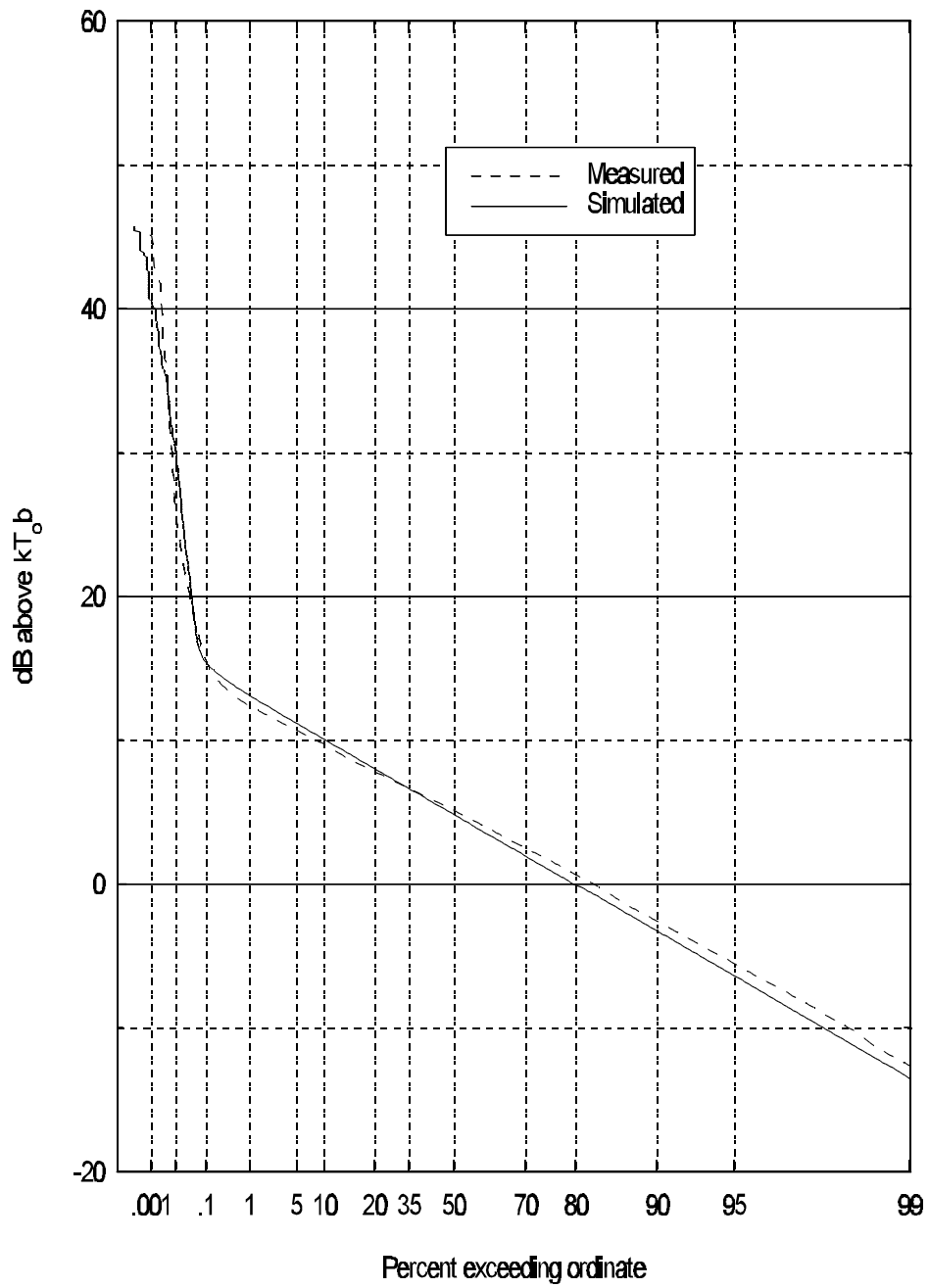


Figure 5.10 Class B noise from measurements in office park on November 30, 1996, from 1:00 to 1:30 p.m.

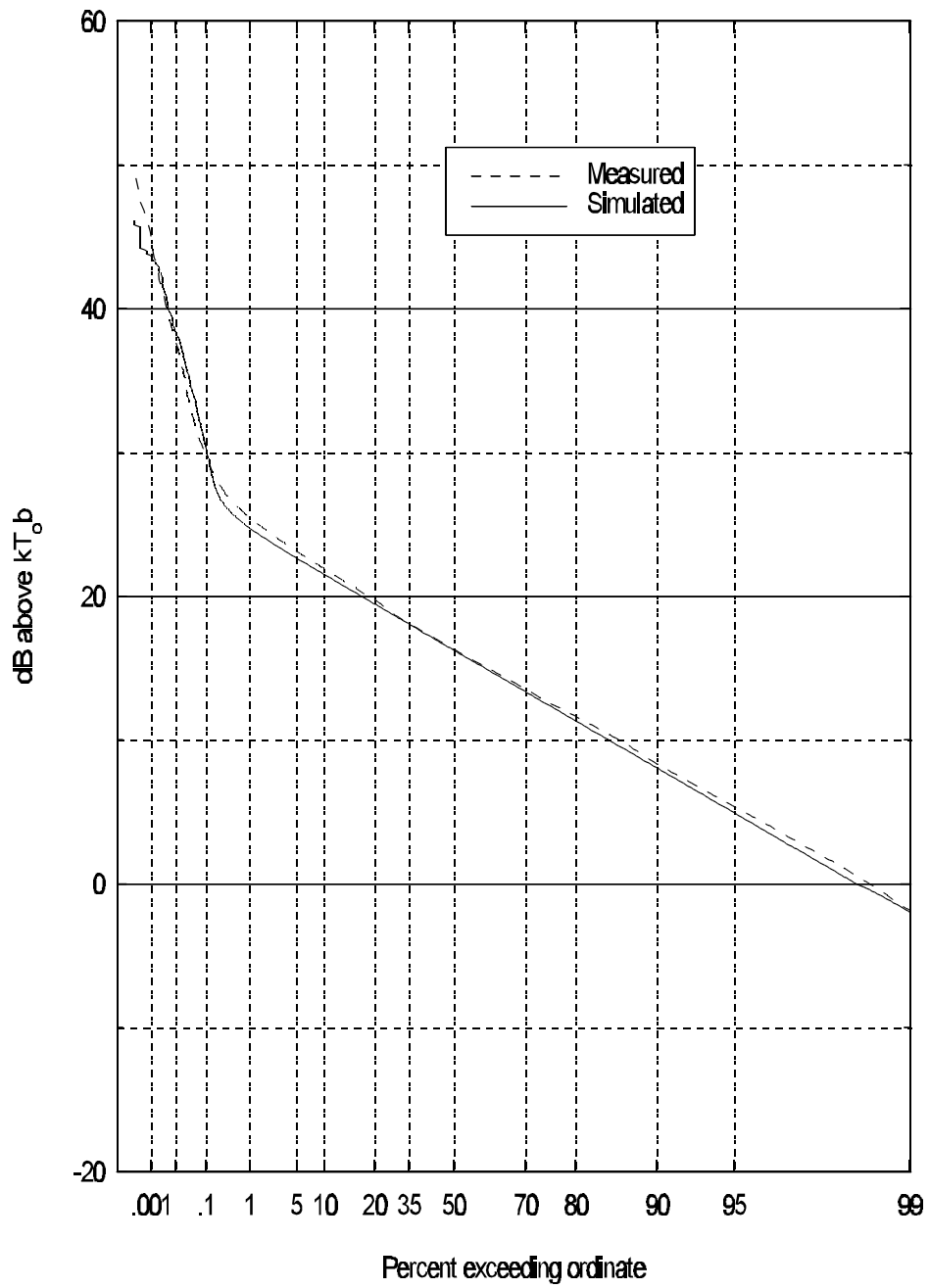


Figure 5.11 Class B noise from measurements in downtown Boulder on November 20, 1996, from 1:00 to 1:30 p.m.

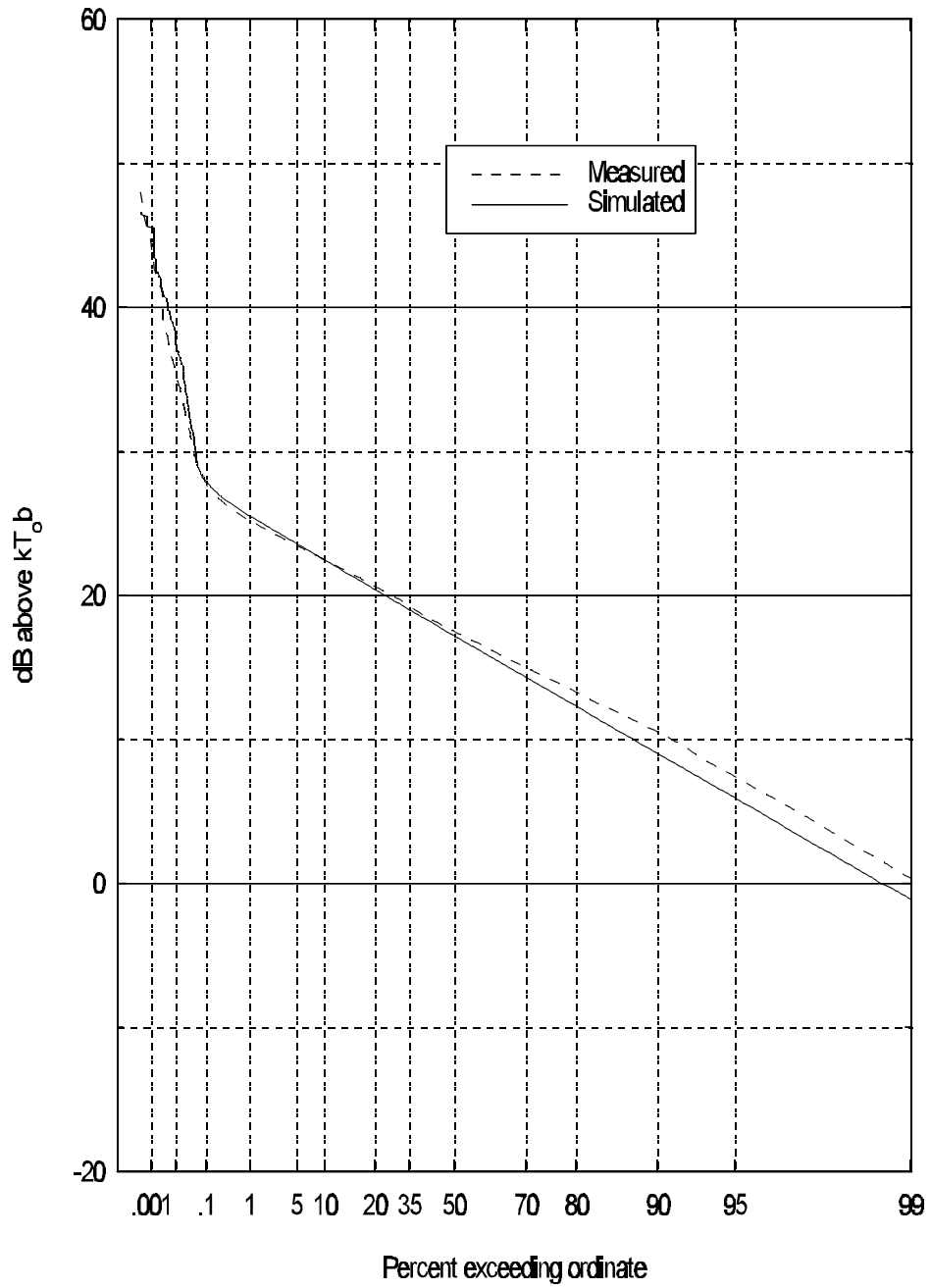


Figure 5.12 Class B noise from measurements in downtown Denver on December 3, 1996, from 11:00 to 11:30 a.m.

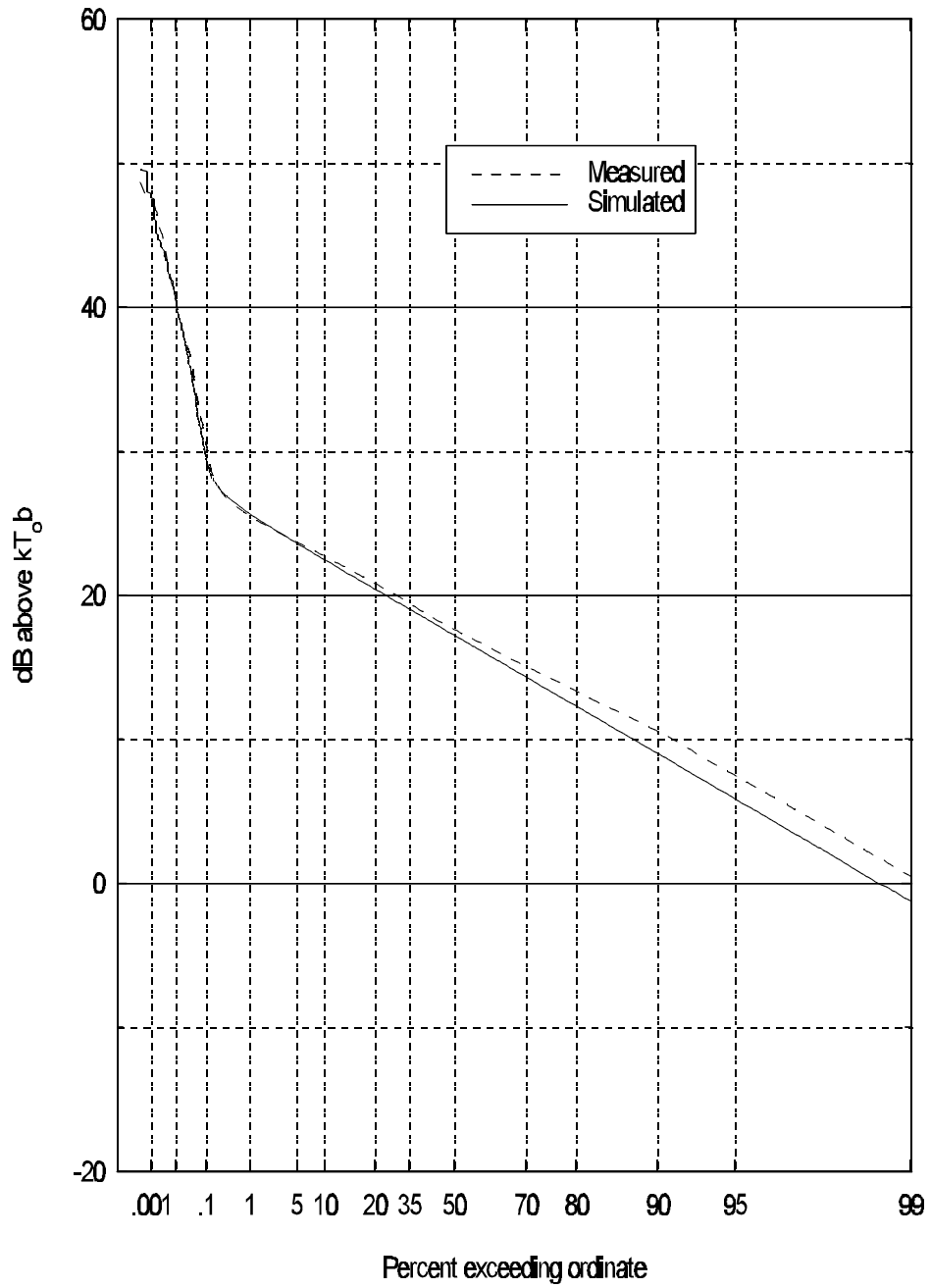


Figure 5.13 Class B noise from measurements in downtown Denver on December 3, 1996, from 11:20 to 11:50 a.m.

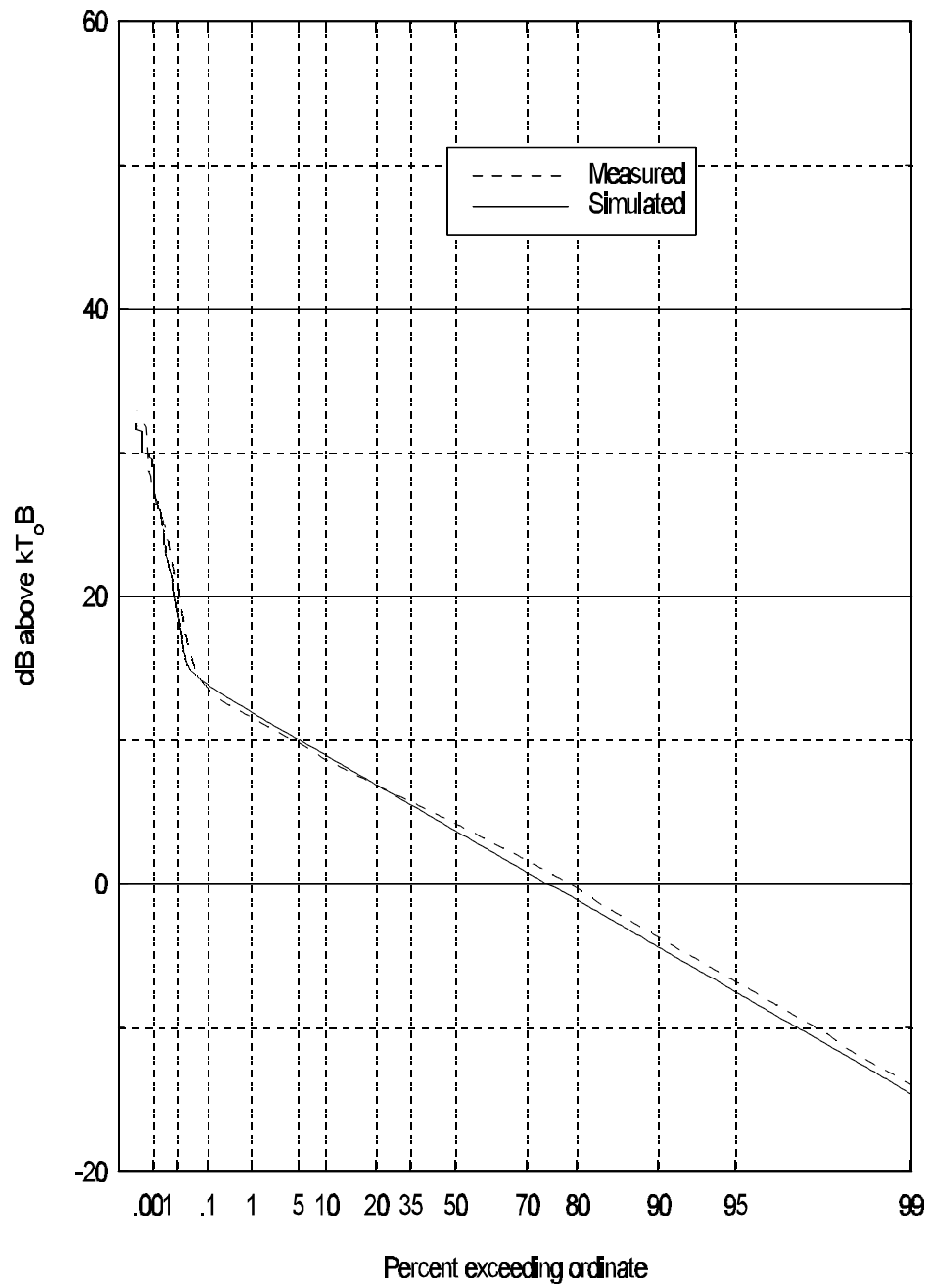


Figure 5.14 Class B noise from automobiles measured in Clear Creek Canyon, Colorado, on December 21, 1996, from 1:00 to 1:30 p.m.

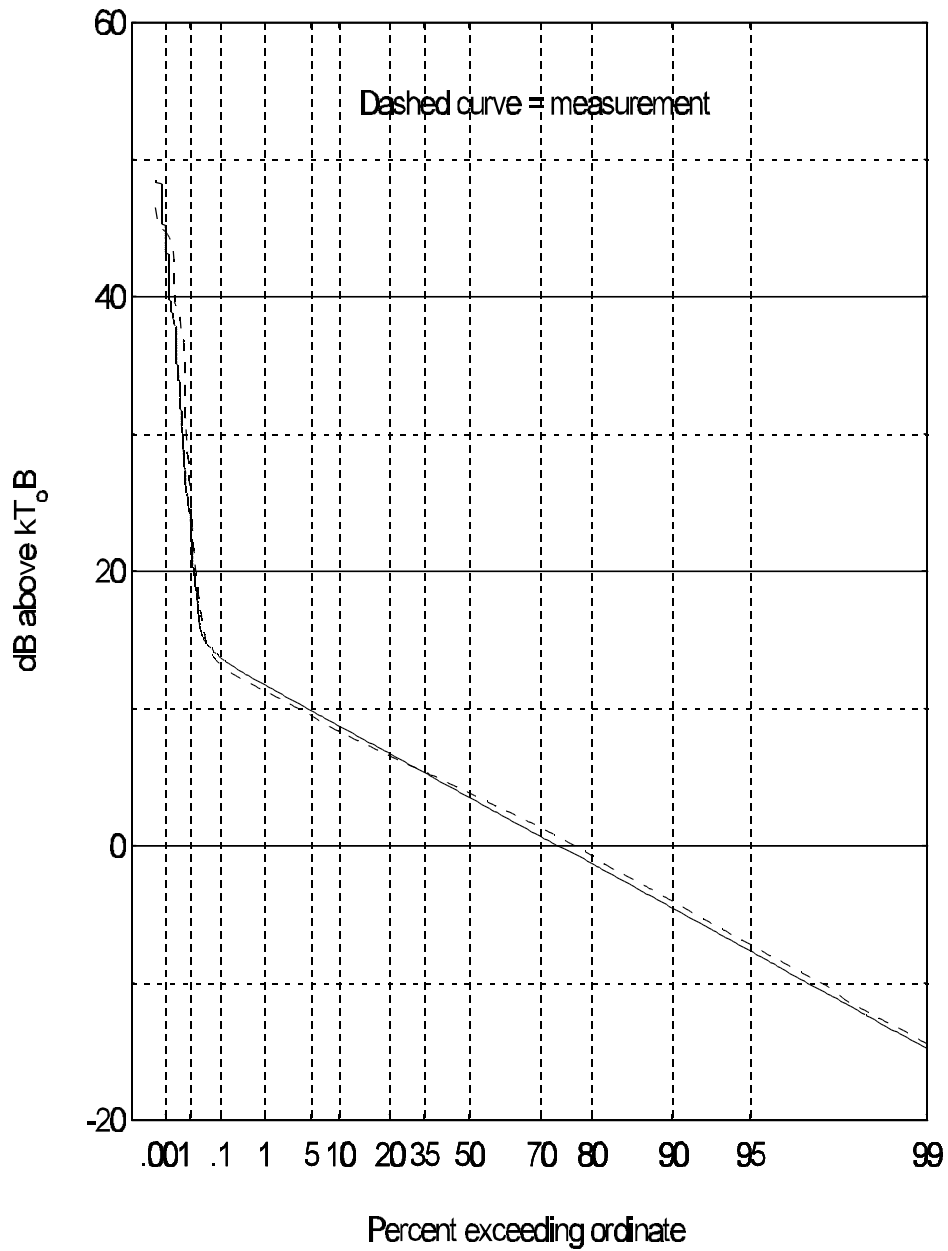


Figure 5.15 Class B noise from automobiles measured in Clear Creek Canyon, Colorado, on December 21, 1996, from 2:00 to 2:30 p.m.

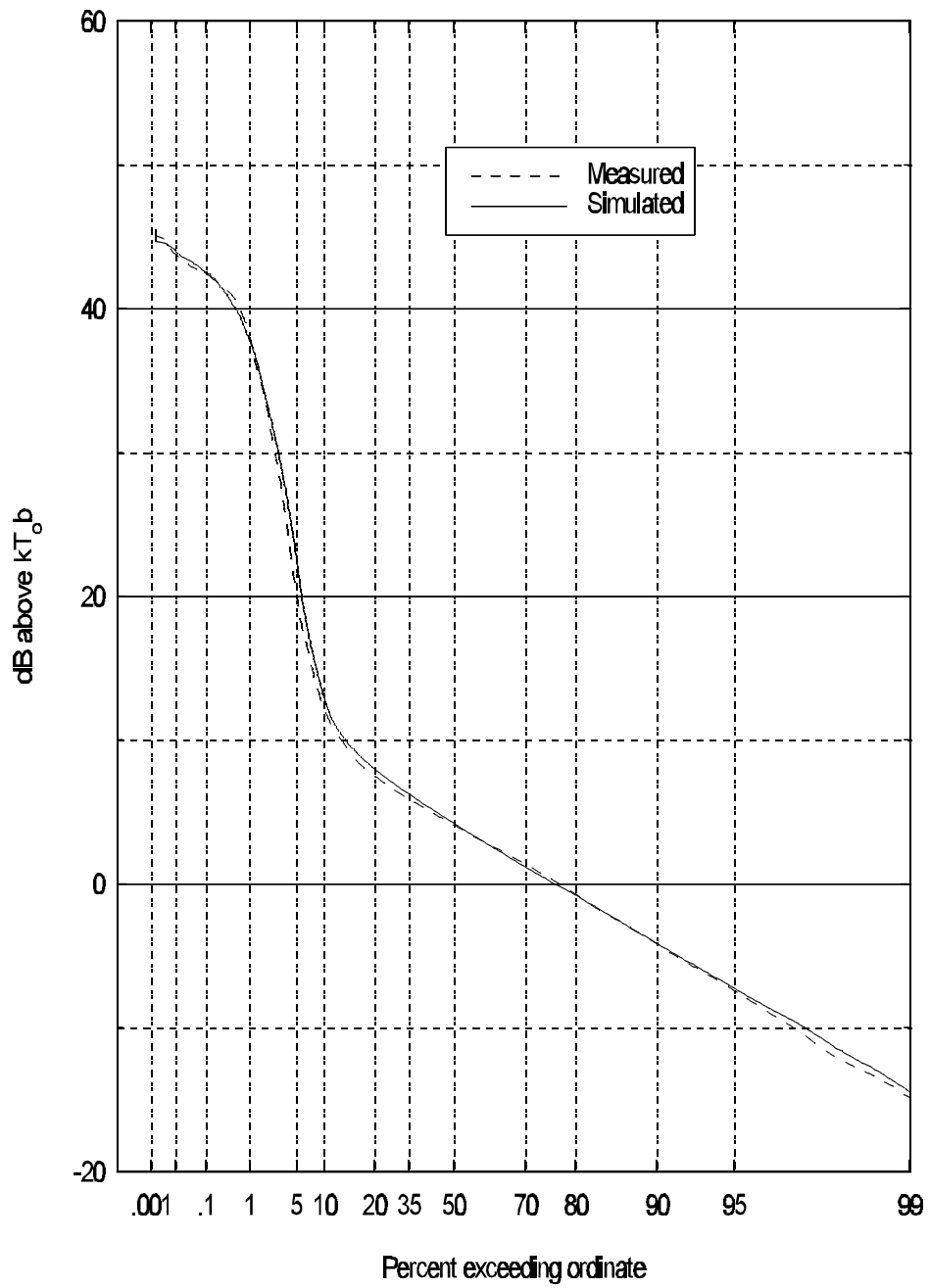


Figure 5.16 Class B noise from electrical network measured near Leyden, Colorado, on November 12, 1996, at 2:02p.m.

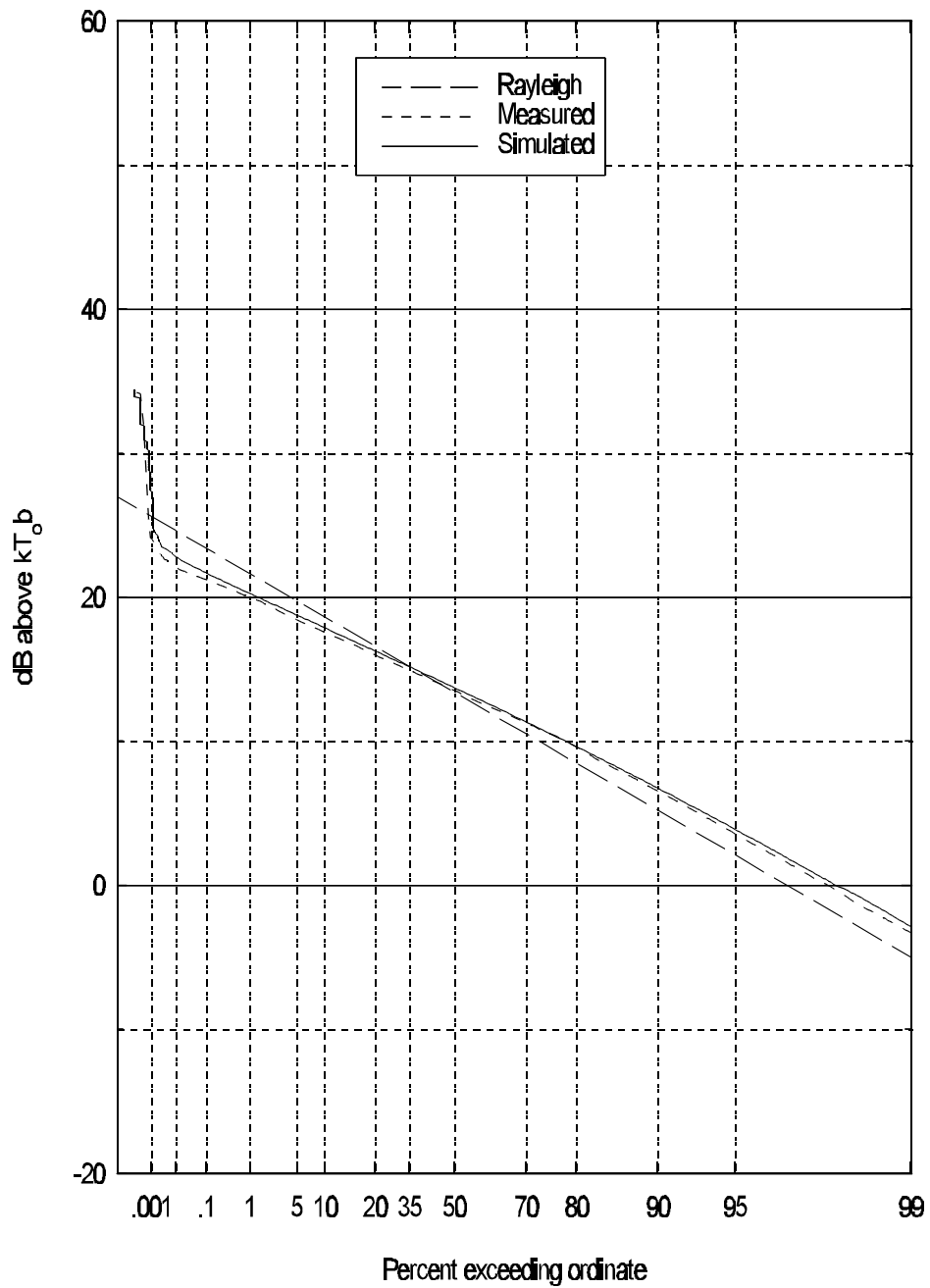


Figure 5.17 Class B noise from measurements in office park on November 27, 1996, from 12:20 to 12:50 a.m.

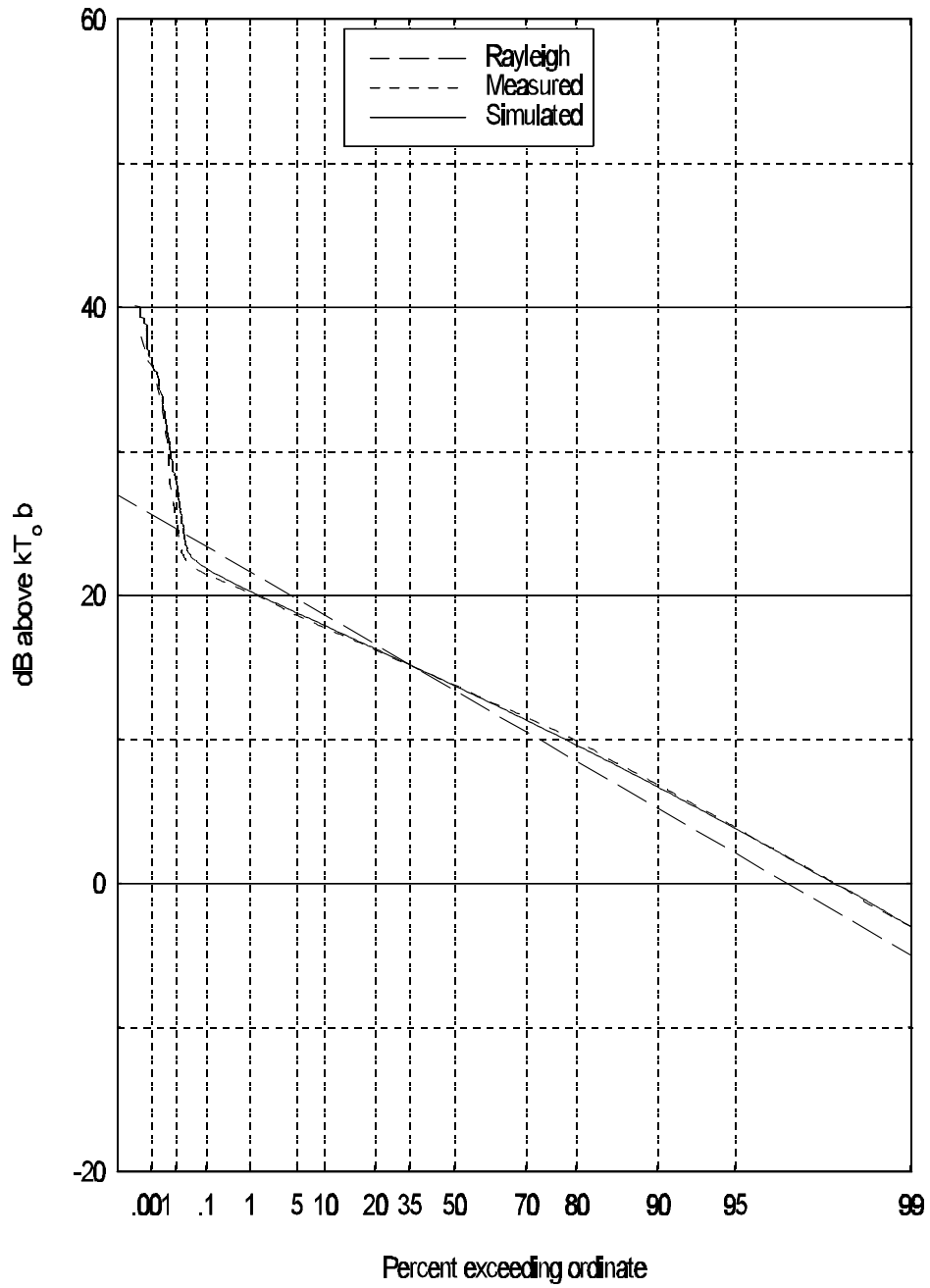


Figure 5.18 Class B noise from measurements in office park on November 27, 1996, from 11:15 to 11:45 a.m.